Formation of an anataselike phase in silica under anisotropic stress: An *ab initio* constant-pressure study

Murat Durandurdu
Department of Physics, University of Texas at El Paso, El Paso, Texas 79968, USA
(Received 8 January 2009; revised manuscript received 14 April 2009; published 2 July 2009)

We study the behavior of α cristobalite under anisotropic stresses using constant-pressure *ab initio* simulations and observe the formation of the anataselike, stishovite, and $CaCl_2$-type structures depending on the degree of hydrostatic compression. These phase transformations proceed via a tetragonal intermediate phase (phase X-I) within $P4_12_12$ symmetry or an orthorhombic intermediate state, having space group of $P2_12_12_1$. The phase transitions into stishovite and the anataselike phase are based on the same intermediate state. The compression of α cristobalite along the c direction produces stishovite while the expansion of α cristobalite along the c direction yields an anataselike phase. The energy-volume calculations suggest that α cristobalite can transform into the anataselike structure if and only if the phase transition into stishovite is suppressed. A phase transition between stishovite and anatase, however, is unlikely to occur.

DOI: 10.1103/PhysRevB.80.024102 PACS number(s): 62.50.−p, 61.50.Ks, 64.70.K−, 91.60.Gf

I. INTRODUCTION

Silica can form many different crystalline modifications (α and β quartz, α and β cristobalite, stishovite, etc.) at ambient temperatures and pressures. Its high-pressure behavior is of great interest because of its wide-ranging implications in geology and materials science and hence, it is a well-studied material.[1–20] Silica shows a complex behavior under pressure and its high-pressure forms strongly depend on the starting structure and experimental procedures. Experimental observations of a number of different high-pressure silica polymorphs yet unidentified have been reported within the last decades.

The behavior of α cristobalite at high pressure has been subject of many experimental and theoretical studies. These investigations have revealed several metastable high-pressure crystalline polymorphs. Experiments showed that α cristobalite transforms into a low symmetric-monoclinic phase around 1.5 GPa.[11,12] Tsuchida and Yagi[13,14] found that α cristobalite converted to phase X-I [or sometimes referred to as cristobalite III (Ref. 15)] at room temperature. The structure of this phase, which had eluded investigators for over a decade, has recently been determined using concurrent molecular-dynamics (MD) simulations and *ab initio* calculations.[16] Upon further increase in pressure above 30 GPa, formation of another phase, X-II (cristobalite IV), was observed, which later was identified as an α-PbO_2-like silica. Upon pressure release, phase X-III was recovered.[13,14] The nature and structure of phase X-III are still unknown. In another investigation, quasihydrostatic compression of α cristobalite[17] led to the formation of a structure similar to stishovite when exceeding 20 GPa.

Constant-pressure simulations have been used to explain the high-pressure behavior of silica. *Cmcm* and stishovite structures were predicted at 16.5 and 23 GPa, respectively, in MD simulations[18] while a direct transition into stishovite at 50 GPa was observed in an *ab initio* MD simulation.[19] In our preceding work,[16] we studied the high-pressure behavior of α cristobalite using both a constant-pressure *ab initio* technique and classical MD simulations, and found that α cristobalite underwent a phase transition into stishovite via an intermediate phase. This intermediate state, which was characterized by a hexagonal close packing of the oxygen sublattice, was identified as the phase X-I. Recent simulations using an empirical potential,[8] on the other hand, suggested that α cristobalite transformed into the anataselike or stishovite phases depending on the loading rate. The authors claimed that the low compression rate resulted in an anataselike structure while a higher compression rate yielded a much higher transition pressure and a phase transformation into stishovite. The anataselike phase was also observed in constant-pressure simulations during pressurizing α quartz, but its formation was interpreted as an unknown artifact of the empirical potential.[9] Currently, it is not known whether the formation of the anataselike phase is due to a limitation of empirical potentials or whether it can really form in silica under some specific conditions. In principle, *ab initio* techniques produce more accurate results and hence, they are ideally suited to eliminate limitations or doubts observed in empirical potentials.

The phase transformation from α cristobalite to anatase proceeds via the Bain path and an expansion along the c direction of α cristobalite produces the anatase structure as a product.[8] Such an observation suggests that the anatase phase might form under nonhydrostatic conditions in which the stress components along [001] direction are less than the others. The behavior of α cristobalite under nonhydrostatic conditions was also explored using constant-pressure simulations and several known or new phases of silica were reported in these studies.[8,10] In this paper, we study α cristobalite under anisotropic stresses; in particular, we try to produce an anatase-type phase under some specific conditions. Our results reveal that α cristobalite can transform into the stishovite, $CaCl_2$-type, and anatase-type phases via the same densification mechanism depending on the degree of hydrostatic compression. Our findings provide different perspectives on high-pressure phases of silica.

II. METHOD

We performed first-principles calculations using the pseudopotential method within the density-functional theory

TABLE I. The structure observed under nonhydrostatic compression of α cristobalite. The stress components $\sigma_{xx}=\gamma_{xx}P$, $\sigma_{yy}=\gamma_{yy}P$, and $\sigma_{zz}=\gamma_{zz}P$, where P and $\gamma_{ii=xx,yy,zz}$ are the applied external pressure and the percentage of the uniaxial stress, respectively.

γ_{xx}	γ_{yy}	γ_{zz}	Gradual phase transformation	First-order phase transformation
1	1	1	Tetragonal $P4_12_12$	Stishovite $P42/mnm$ (40 GPa)
1	1	0.95	Tetragonal $P4_12_12$	Stishovite $P42/mnm$ (40 GPa)
0.9	1	0.9	Orthorhombic $P2_12_12_1$	Stishovite $P42/mnm$ (40 GPa)
1	1	0.9	Tetragonal $P4_12_12$	Anatase $I4_1/amd$ (40 GPa)
0.85	1	0.9	Orthorhombic $P2_12_12_1$	Anatase $I4_1/amd$ (40 GPa)
1	1	0.8	Tetragonal $P4_12_12$	Anatase $I4_1/amd$ (30 GPa)
0.9	1	0.95	Orthorhombic $P2_12_12_1$	$CaCl_2$-type $Pnnm$ (50 GPa)

(DFT) formalism and the generalized gradient approximation (GGA) of Perdew-Bucker and Ernzerhof[21] to evaluate the exchange-correlation energy. The calculations were carried out using SIESTA,[22] a DFT code that uses a linear combination of atomic orbitals as the basis set and norm-conserving Troullier-Martins pseudopotentials.[23] An optimized split-valence double ξ plus polarized basis set was employed. A uniform mesh with a plane-wave cutoff of 120 Ry was used to present the electron density, the local part of the pseudopotential, and the Hartree and the exchange-correlation potential. The simulation cell consists of 96 atoms with periodic boundary conditions. We used Γ-point sampling for the supercell's Brillouin-zone integration, which is reasonable for a cell with 96 atoms. For nonhydrostatic compressions, we set the stress components $\sigma_{xx}=\gamma_{xx}P$, $\sigma_{yy}=\gamma_{yy}P$, and $\sigma_{zz}=\gamma_{zz}P$, where P and $\gamma_{ii=xx,yy,zz}$ are the applied external pressure and the percentage of the uniaxial stress, respectively. Pressure was increased by an increment of 10 GPa. For each value of the applied pressure, the lattice vectors and the atomic positions were optimized together until the stress tolerance was less than 0.5 GPa and the maximum atomic force was smaller than 0.01 eV $Å^{-1}$. For minimization of geometries, a variable-cell shape conjugate-gradient method under a constant pressure was used. For the energy-volume calculations, we considered the unit cell for SiO_2 phases. The Brillouin-zone integration was performed with automatically generated $6\times6\times6$ k-point mesh for the phases following the convention of Monkhorst and Pack.[24] In order to determine symmetry of the high-pressure phases formed in the simulations, we used the KPLOT program[25] that provides detailed information about space group, cell parameters, and atomic position of a given structure. For the symmetry analysis, we used 0.1 Å, 4°, and 0.7 Å tolerances for bond lengths, bond angles, and interplanar spacing, respectively.

III. RESULTS

In order to investigate the influence of the degree of the hydrostaticity on the phase transformation of α cristobalite, we consider six different anisotropic stresses along different directions. For all cases studied here, we start our simulations from α cristobalite. We summarize our results in Table I. The volume changes under these loading conditions and pure hydrostatic pressure are represented in Fig. 1. As seen from the figure, α cristobalite shows practically identical equation of state in the pressure range from 0–20 GPa. At higher pressures, as expected, it presents quite different equation of state and undergoes a first-order phase transition at different pressures. We should note here that the use of relatively larger pressure increase (10 GPa) does not allow us to precisely predict the influence of the degree of hydrostaticity on the critical pressures.

As seen from Table I, we observe the formation of the stishovite, $CaCl_2$-type, and anataselike structures owing to the first-order phase transformation. In stishovite, each SiO_6 octahedra shares corners with eight neighbors and shares edges with two other neighbors, forming a linear chain. On the other hand, in anatase, each SiO_6 octahedra shares corners with four neighbors and shares edges with four other neighbors, forming a zigzag chain with a screw axis. Therefore, anatase is less dense than stishovite, which is clearly observed in our simulations (see Fig. 1) and the energy-volume calculations (see below). The $CaCl_2$-type phase is a distorted stishovite phase and a result of rotation of the SiO_6 octohedra relative to each other about the c axis.

The stishovite and $CaCl_2$-type crystals are known phases of SiO_2, but the anataselike phase in this material has not been observed experimentally so far. On the other hand, the present simulations demonstrate that it is possible to prepare

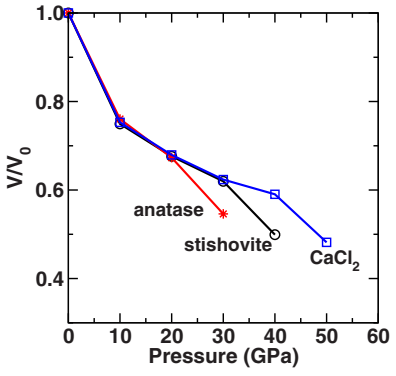

FIG. 1. (Color online) Volume change under hydrostatic and nonhydrostatic compressions. For clarity, we only plot three conditions: (i) pure hydrostatic pressure (stishovite is formed), (ii) $\sigma_{xx}=P$, $\sigma_{yy}=P$, $\sigma_{zz}=0.8P$ (the anataselike phase is formed), and (iii) $\sigma_{xx}=0.9P$, $\sigma_{yy}=P$, and $\sigma_{zz}=0.95P$ ($CaCl_2$-type phase is formed).

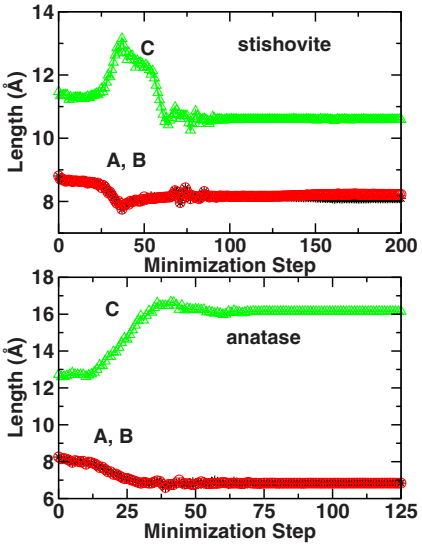

FIG. 2. (Color online) The modification of simulation cell lengths as a function of minimization step during the evolution of the stishovite and anataselike phases.

this phase experimentally as a metastable phase under nonhydrostatic pressure by simply applying a 5–10 % less stress along the c direction, relative to the other directions.

In order to determine how the densification mechanism occurs for these phase transformations, we carefully analyze each structure using KPLOT program. The analyses suggest that α cristobalite gradually transforms into the tetragonal phase within the $P4_12_12$ symmetry (phase XI) or an orthorhombic intermediate phase having the space group $P2_12_12_1$ (for the cases $\sigma_{xx} \neq \sigma_{yy}$). For both the phases, the densification mechanism is practically identical and is due to a close-packing anion sublattice, i.e., a slightly distorted hexagonal close-packed anion sublattice. All forms of silica observed in the present study can, indeed, be considered as a hexagonal close-packed anion sublattice with cations located in tetrahedral or octahedral interstices except anataselike phase that can be described by its cubic close-packed (fcc) arrangement for the oxygen sublattice. These observations basically suggest that the densification in α cristobalite occurs in two steps: anions form close packing first, followed by reconstructive phase transforms into higher coordinated phases.

In simulations, we can also easily track the transformation mechanism of these phase changes by simply analyzing the simulation cell vectors or the motion of the atomic coordinates. In Fig. 2, we plot the simulation cell lengths at 40 GPa for the pure hydrostatic pressure and the nonhydrostatic case ($\sigma_{xx}=P$, $\sigma_{yy}=P$, and $\sigma_{zz}=0.9P$, where $P=40$ GPa) as a function of minimization step. The simulation cell is initially oriented such that its lattice vectors **A**, **B**, and **C** are along the [100], [010], and [001] directions, respectively. The magnitude of these vectors is plotted in the figure. During both phase transformations, the variation in simulation cell angles less than 1.5° and hence, the influence of shear deformation on these phase transformations is very small. As can be seen from the figure, the phase transformation into stishovite phase occurs in two steps: first the cell lengths decouple with two lengths decreasing (along [100] and [010] axes) with a corresponding increase in the third length (along [001] axis); secondly, the structure is noticeably compressed along the c direction while it is expanded slightly along the other directions. On the other hand, the transformation into the anatase phase proceeds in one step, and it is associated with a simultaneous expansion along the c direction and a compression along the other directions. In order to form the stishovite structure, the Si atoms make new bonds with O atoms at the adjunct [001] planes and the SiO_4 tetrahedra rotate while to structure the anataselike state, Si atoms form new bonds with O atoms at the same planes and the transformation does not involve any rotation of SiO_4 tetrahedra. Nevertheless, a careful structural analysis using the KPLOT program suggests that both phase transformations proceed via the same intermediate state having the $P4_12_12$ tetragonal symmetry. For the nonhydrostatic cases $\sigma_{xx} \neq \sigma_{yy}$, the variation in the simulation cell lengths is also very similar except that the $|\mathbf{A}|$ and $|\mathbf{B}|$ lengths noticeably deviate from each other. This, of course, yields an orthorhombic intermediate state within $P2_12_12_1$ symmetry rather than the tetrahedral one.

The modifications of the simulation cell vectors imply that the mechanism of these phase transitions is very simple and can be pictured in terms of the movements of atoms along the [001] directions. The evolution of the stishovite and anataselike phases are presented in Fig. 3.

In order to shed some light on these phase transitions, we also study the total energy of the α cristobalite, anatase, and stishovite phases as a function of volume and fit their energy-volume relations to the third-order Birch-Murnaghan equation of state. The computed total energies per molecule as a function of volume are given in Fig. 4. The molar volume of the anataselike phase is less than that of the stishovite phase, which is in good agreement with the previous density-functional calculations.[9] However, the energy difference between α cristobalite and anatase states is larger than the energy difference between α cristobalite and stishovite. This result suggests that the formation of anatase is not energetically favorable relative to stishovite, but it can occur in silica if the phase transition into stishovite is suppressed. When the common tangent lines are considered between these phases, we can see that there is no phase transition between anatase and stishovite under hydrostatic pressure. Furthermore, the energy-volume relations suggest that the α-cristobalite-to-anataselike phase transformation should occur at a higher transition pressure than the α-cristobalite-to-stishovite phase transformation under pure hydrostatic pressure.

IV. CONCLUSIONS

In summary, we study the response of α cristobalite to nonhydrostatic compressions using *ab initio* constant-pressure simulations and explore the formation of the anataselike phase in addition to the common silica phases, stishovite, and $CaCl_2$ type. Before transforming into a high coordinated phase, α cristobalite gradually transforms into a tetragonal phase (phase X-I) or an orthorhombic phase, depending on degree of hydrostaticity. The densification mechanism under hydrostatic and nonhydrostatic stresses ap-

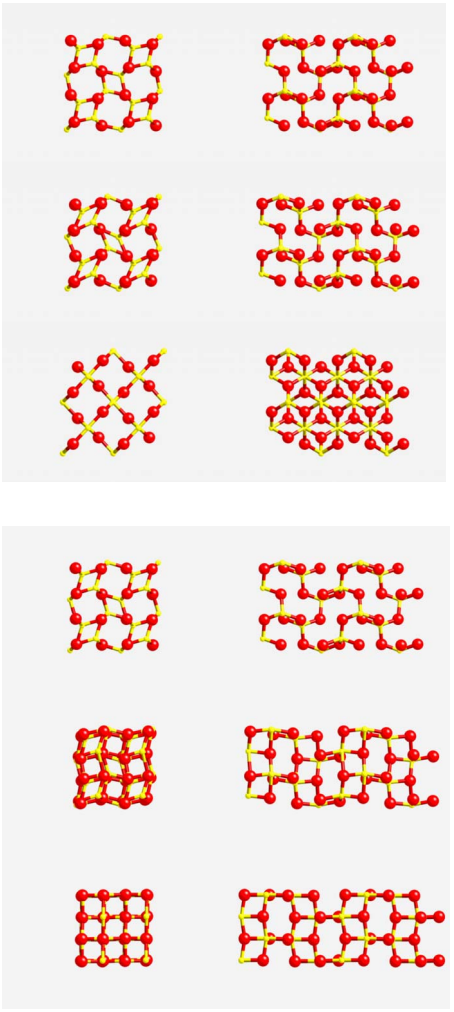

FIG. 3. (Color online) The evolution of the stishovite and anataselike phases.

pears to be the same and is associated with a closed-packed hexagonal anion sublattice. The transformation into stishovite or anataselike phase proceeds the same intermediate phase. The energy-volume calculations also suggest a possible phase transformation into the anataselike phase, but this phase transformation occurs if and only if the transformation into stishovite phase is suppressed. Although the anataselike phase in silica has not been observed in any experiment, our

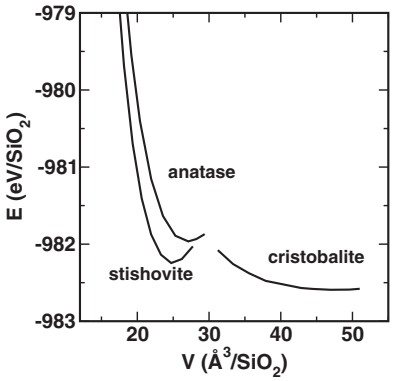

FIG. 4. Energy-volume curves of the α cristobalite, stishovite, and anataselike structures.

simulations suggest that it can form under some specific conditions (by simply applying a 5–10 % less stress along the c direction, relative to the other directions) and that it is not energetically favorable under hydrostatic pressure relative to stishovite, in a contrast to the MD simulations based on an empirical potential.[8] Our findings might help experimentalists to set up experimental procedures that might produce this transformation. Using recently developed experimental techniques for controlling and measuring the three-dimensional distribution of stress and strain in samples under pressure[26,27] or newly developed, the simultaneous application of uniaxial stress and hydrostatic pressure techniques[28] might be helpful in synthesizing the anataselike phase, and in understanding the behavior of α cristobalite under nonhydrostatic compressions. We should note here that all our calculations were performed at zero temperature (relaxation of the structures at constant pressure) and hence, no thermal motions were taken account. In reality, temperature is known to have a large influence on the pressure-induced phase transformations of this system and hence, the combination of temperature and nonhydrostatic stresses might produce different phase changes in experiments. The challenge now goes to the experimentalist to probe this phase of such an important material.

ACKNOWLEDGMENTS

The calculations were run on SACAGAWEA, a 128 processor BEOWULF cluster, at the University of Texas at El Paso.

[1] K. J. Kingma, C. Meade, R. J. Hemley, H. K. Mao, and D. R. Veblen, Science **259**, 666 (1993).
[2] D. M. Teter, R. J. Hemley, G. Kresse, and J. Hafner, Phys. Rev. Lett. **80**, 2145 (1998).
[3] A. El Goresy, L. Dubrovinsky, T. G. Sharp, S. K. Saxena, and M. Chen, Science **288**, 1632 (2000).
[4] S. R. Shieh, T. S. Duffy, and B. Li, Phys. Rev. Lett. **89**, 255507 (2002).
[5] L. S. Dubrovinsky, S. K. Saxena, P. Lazor, R. Ahuja, O. Eriksson, J. M. Wills, and B. Johansson, Nature (London) **388**, 362 (1997).
[6] Y. Tsuchida and T. Yagi, Nature (London) **340**, 217 (1989).
[7] J. Haines, J. M. Léger, F. Gorelli, and M. Hanfland, Phys. Rev. Lett. **87**, 155503 (2001).
[8] Y. Liang, C. R. Miranda, and S. Scandolo, Phys. Rev. Lett. **99**, 215504 (2007).
[9] R. Martoňák, D. Donadio, A. R. Oganov, and M. Parrinello, Nature Mater. **5**, 623 (2006); Phys. Rev. B **76**, 014120 (2007).
[10] D. Donadio, R. Martoňák, P. Raiteri, and M. Parrinello, Phys. Rev. Lett. **100**, 165502 (2008).

[11] D. C. Palmer and L. W. Finger, Am. Mineral. **79**, 1 (1994).
[12] D. C. Palmer, R. J. Hemley, and C. T. Prewitt, Phys. Chem. Miner. **21**, 481 (1994).
[13] Y. Tsuchida and T. Yagi, Nature (London) **347**, 267 (1990).
[14] Y. Yahagi, T. Yagi, H. Yakamawaki, and K. Aoki, Solid State Commun. **89**, 945 (1994).
[15] R. J. Hemley, C. T. Prewitt, and K. J. Kingma, Rev. Mineral. **29**, 41 (1994).
[16] L. Huang, M. Durandurdu, and J. Kieffer, Nature Mater. **5**, 977 (2006).
[17] M. Yamakata and T. Yagi, Proc. Jpn. Acad., Ser. B: Phys. Biol. Sci. **73**, 85 (1997).
[18] S. Tsuneyuki, Y. Matsui, H. Aoki, and M. Tsukada, Nature (London) **339**, 209 (1989).
[19] D. D. Klug, R. Rousseau, K. Uehara, M. Bernasconi, Y. Le Page, and J. S. Tse, Phys. Rev. B **63**, 104106 (2001).
[20] J. Badro, J. L. Barrat, and P. Gillet, Phys. Rev. Lett. **76**, 772 (1996).
[21] J. P. Perdew, K. Burke, and M. Ernzerhof, Phys. Rev. Lett. **77**, 3865 (1996).
[22] P. Ordejón, E. Artacho, and J. M. Soler, Phys. Rev. B **53**, R10441 (1996).
[23] N. Troullier and J. L. Martins, Phys. Rev. B **43**, 1993 (1991).
[24] H. J. Monkhorst and J. D. Pack, Phys. Rev. B **13**, 5188 (1976).
[25] R. Hundt, J. C. Schön, A. Hannemann, and M. Jansen, J. Appl. Crystallogr. **32**, 413 (1999).
[26] H. K. Mao, J. Shu, Y. Fei, J. Hu, and R. J. Hemley, Phys. Earth Planet. Inter. **96**, 135 (1996).
[27] R. J. Hemley, H. K. Mao, G. Shen, J. Badro, P. Gillet, M. Hanfland, and D. Häusermann, Science **276**, 1242 (1997).
[28] H. D. Hochheimer, F. Widulle, J. Th. Held, G. Strehl, R. T. Kotitschke, and A. R. Adams, High Press. Res. **18**, 41 (2000).